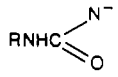

portions of the tolbutamide and chlorpropamide ligands in I and III and the relatively short HN–C distances at 1.35 (2) Å (Table VII). In addition the R–NH–C angles in both complexes are nearly 120° (Table VII) suggesting sp^2 hybridization around the NHR nitrogen. The contribuiton of resonance form 3 is reminiscent of the

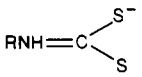

form in dithiocarbamate complexes, which is responsible for the ability of the latter to stabilize high oxidation states in certain metals. By analogy the sulfonylurea ligands might possess similar coordination properties and be capable of supporting certain high oxidation states. This aspect of the coordination chemistry of sulfonylurea drugs is also being pursued in our laboratories.

Acknowledgment. We are indebted to Professor D. Coucouvanis for use of his X-ray diffraction equipment in the course of this study. We also thank Danae Christodoulou for assistance.

Supplementary Material Available: Tables of final atomic and thermal parameters for $Hg(CH_3C_6H_4SO_2NCONH\text{-}n\text{-}Bu)_2$ and $K[Cd(ClC_6H_4SO_2NCONH\text{-}n\text{-}Pr)_3]$ and a stereoview and a drawing of $K[Cd(ClC_6H_4SO_2NCONH\text{-}n\text{-}Pr)_3]$ with anisotropic temperature factors shown (5 pages); tables of structure factors $(10|F_o|/F_c)$ (18 pages). Ordering information is given on any current masthead page.

Contribution from the Gray Freshwater Biological Institute, University of Minnesota, Navarre, Minnesota 55392, Department of Chemistry, University of Minnesota, Minneapolis, Minnesota 55455, and Department of Chemistry, Cornell University, Ithaca, New York 14853

Mössbauer and EPR Spectroscopy of Catechol 1,2-Dioxygenase

T. A. Kent,[1a] E. Münck,*[1a] J. W. Pyrz,[1b] J. Widom,[1c] and L. Que*[1b]

Received July 1, 1986

Mössbauer and EPR studies of catechol 1,2-dioxygenase from *Pseudomonas putida* and several of its complexes show that the iron center is high-spin ferric in character in all these complexes, including the enzyme–catechol complex and the steady-state intermediate obtained from the reaction of the enzyme, pyrogallol, and O_2. The Mössbauer spectrum of the native enzyme consists of two major components whose relative amounts vary with pH and buffer. One component exhibits a spectrum virtually identical with those of protocatechuate 3,4-dioxygenases from *Pseudomonas aeruginosa* and *Brevibacterium fuscum* with a common magnetic hyperfine constant, $A/g_n\beta_n$, of −21.0 T. This A value appears to be characteristic of this class of dioxygenases. It is closely matched by that of Fe(salen)benzoate (−20.9 T), a synthetic complex that approximates the coordination environment of the metal site. The binding of substrate and inhibitors alters the observed magnetic hyperfine parameters and zero-field splittings. $A/g_n\beta_n$ changes for −20.8 T for the phenol complex to −20.0 T for the thiophenol complex, indicating the greater covalency of the Fe–S bond. More interestingly, $A/g_n\beta_n$ for the catechol complex, −18.9 T, is the smallest in magnitude observed for a dioxygenase complex and indicates a greater delocalization of unpaired spin density away from the ferric center than in the phenol and thiophenol complexes. The unpaired spin density is presumably transferred onto the catechol, and this may enhance the reactivity of the substrate with dioxygen.

Introduction

Catechol 1,2-dioxygenase (catechol:oxygen 1,2-oxidoreductase (decyclizing); EC 1.13.11.1; CTD) from *Pseudomonas putida* is a non-heme iron enzyme that catalyzes the oxidative cleavage of catechols to *cis,cis*-muconic acids with the incorporation of the elements of dioxygen into the carboxylate functions of the product.[2] The enzyme has a molecular mass of 63 000 and consists of two nonidentical subunits of mass 30 000 and 32 000 and one iron.[3] It exhibits a visible absorption spectrum with an absorbance maximum near 460 nm ($\epsilon \sim 3500\ M^{-1}\ cm^{-1}$), which arises from tyrosinate-to-Fe(III) charge-transfer transitions.[4,5] CTD belongs to an emerging class of proteins exhibiting metal phenolate coordination, which also includes the transferrins, the purple acid phosphatases, and protocatechuate 3,4-dioxygenase (PCD).[6]

PCD catalyzes a reaction similar to that of CTD. Mössbauer studies of PCD (from *Pseudomonas aeruginosa* and *Brevibacterium fuscum*), its enzyme–substrate complex, and a steady-state intermediate generated upon oxygenation have shown that the active site iron remains high-spin ferric in these three forms.[7,8] These observations plus the persistence of the phenolate-to-Fe(III) charge-transfer band in transient intermediates[9,10] suggest that the charge and spin state of the iron are unchanged throughout the catalytic cycle. Thus a novel oxygenase mechanism in which the iron serves to activate substrate rather than O_2 has been proposed for these dioxygenases.[11] We report here a Mössbauer and EPR study of catechol 1,2-dioxygenase and several of its complexes, which shows that the iron center is high-spin ferric in these complexes, corroborating the earlier PCD studies.[7,8]

Data are also presented for the synthetic complex, Fe(salen)-BzO,[12] which exhibits Mössbauer parameters quite similar to those

(1) (a) Gray Freshwater Biological Institute, University of Minnesota. (b) Department of Chemistry, University of Minnesota. (c) Cornell University.
(2) (a) Que, L., Jr. *Adv. Inorg. Biochem.* **1983**, *5*, 167–199. (b) Nozaki, M. *Top. Curr. Chem.* **1979**, *78*, 145–186.
(3) Nakai, C.; Kagamiyama, H.; Saeki, Y.; Nozaki, M. *Arch. Biochem. Biophys.* **1979**, *195*, 12–22.
(4) Kojima, Y.; Fujisawa, H.; Nakazawa, A.; Nakazawa, T.; Kanetsuna, F.; Taniuchi, H.; Nozaki, M.; Hayaishi, O. *J. Biol. Chem.* **1967**, *242*, 3270–3278.
(5) (a) Que, L., Jr.; Heistand, R. H. II. *J. Am. Chem. Soc.* **1979**, *101*, 2219–2221. (b) Que, L., Jr.; Heistand, R. H. II; Mayer, R.; Roe, A. L. *Biochemistry* **1980**, *19*, 2588–2593.
(6) Que, L., Jr. *Coord. Chem. Rev.* **1983**, *50*, 73–108.
(7) Que, L., Jr.; Lipscomb, J. D.; Zimmermann, R.; Münck, E.; Orme-Johnson, N. R.; Orme-Johnson, W. H. *Biochim. Biophys. Acta* **1976**, *452*, 320–334.
(8) Whittaker, J. W.; Lipscomb, J. D.; Kent, T. A.; Münck, E. *J. Biol. Chem.* **1984**, *259*, 4466–4475.
(9) Bull, C.; Ballou, D. P.; Otsuka, S. *J. Biol. Chem.* **1981**, *256*, 12681–12686.
(10) Walsh, T. A.; Ballou, D. P.; Mayer, R.; Que, L., Jr. *J. Biol. Chem.* **1983**, *258*, 14422–14427.
(11) Que, L., Jr.; Lipscomb, J. D.; Münck, E.; Wood, J. M. *Biochim. Biophys. Acta* **1977**, *485*, 60–74.

0020-1669/87/1326-1402$01.50/0

of the dioxygenases in the native state.

Experimental Section

^{57}Fe-enriched CTD was purified from *P. putida* (*Pseudomonas arvilla* C-1, ATCC 23974) cells that had been grown on ^{57}Fe (1 mg/L of culture medium) according to a modification of the procedure of Fujiwara et al.[13,14] The enzyme thus obtained had a specific activity of 25–30 units/mg and an iron content of 0.9 mol of Fe/mol of enzyme. Changes of buffer were effected by passage through a Pharmacia PD-10 column; the effluent was then concentrated with a Minicon concentrator. The various complexes were generated by the addition of the appropriate amount of ligand to the concentrated enzyme solution. The steady-state intermediate from the reaction of CTD with pyrogallol and O_2[15] was prepared by adding pyrogallol to a 0.5 mM solution of CTD that had been previously saturated with O_2 at 2 °C. Within 30 s the enzyme solution turned gold in color, indicating the formation of the intermediate, and the solution was transferred to the Mössbauer cell and frozen at 77 K within 60 s of mixing.

^{57}Fe(salen)BzO was obtained by adding a slight excess of benzoic acid to a CH_2Cl_2 solution of $[^{57}Fe(salen)]_2O$, prepared according to published methods.[16] A 9:1 toluene/CH_2Cl_2 solution of the complex, which yielded a glass upon freezing in liquid N_2, was used for the present study.

The EPR data were recorded in J. D. Lipscomb's laboratory (University of Minnesota) on a Varian E-109 spectrometer equipped with an Oxford Instruments low-temperature cryostat. The Mössbauer spectra were recorded as described previously.[17] The Mössbauer samples were enriched in ^{57}Fe (New England Nuclear) and approximately 1 mM in protein concentration.

A Data General NOVA 4S minicomputer was used to simulate the Mössbauer spectra. The paramagnetic properties of magnetically dilute high-spin ferric complexes may be approximated by a $S = {}^5/_2$ spin Hamiltonian

$$H_e = D\left[S_z^2 - \frac{35}{12} + \frac{E}{D}(S_x^2 - S_y^2)\right] + 2\beta\vec{H}_{app}\cdot\vec{S} \qquad (1)$$

where β is the Bohr magneton and $\vec{H}_{app}$ is the applied field. The term in brackets approximates the splitting of the ^{6}S ground multiplet into three Kramers doublets. The interpretation of EPR and Mössbauer data in terms of D and E/D has been discussed in detail elsewhere.[18-20] For high-spin ferric complexes the orbital moment is essentially zero and in weak applied fields ($g\beta H_{app} \ll D$) the g values are given by

$$g_{ij} = 4\langle S_{ij}\rangle \qquad i = 1\text{–}3 \qquad j = x, y, \text{ or } z \qquad (2)$$

where i refers to a particular doublet and j one of the axes defined by H_e. Doublet 1 is the ground doublet, 2 is the middle doublet, and 3 is the uppermost doublet. $\langle S_{ij}\rangle$ is the expectation value of the spin for the ith doublet when $\vec{H}_{app}$ is along the jth direction, x, y, or z. Given D, E/D, and $\vec{H}_{app}$, $\langle S_{ij}\rangle$ can be calculated from eq 1.

The hyperfine interactions between the unpaired electrons and the ^{57}Fe nucleus were calculated by using standard techniques.[20] For magnetically dilute high-spin ferric complexes at temperatures below ~20 K the electronic relaxation rate is slow compared with the nuclear precession frequency. For small H_{app} the observed Mössbauer spectrum will have three components each corresponding to one Kramers doublet. The shape of each spectral component will be dominated by the internal field produced by that doublet, namely

$$\vec{H}_{int} = -\frac{A\cdot\langle\vec{S}\rangle}{g_n\beta_n} \qquad (3)$$

We assume A is a scalar. The relative intensities of the three component spectra are determined by the thermal populations of the doublets. Note that when the induced moment of the electronic ground state is extremely anisotropic, an unusually large number of grid points must be used in the powder average. Otherwise, artifacts will cause systematic errors in zero-field splitting determinations.

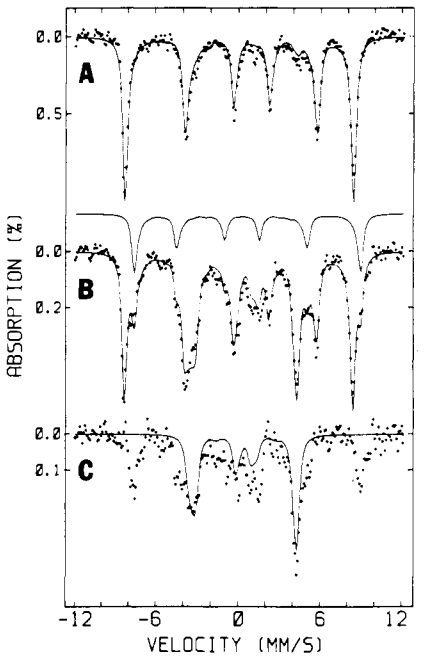

Figure 1. Mössbauer spectra of CTD + benzoate (100 mM) in 50 mM HEPES (pH 7.5) recorded with a 0.06-T field parallel to the γ-beam: (A) spectrum at 1.3 K; (B) spectrum at 10 K; (C) difference spectrum as described in text. The simulations (solid curves) were calculated from eq 1 and 3. The curves through the data in parts A and B represent the contributions of all three Kramers doublets. The curve in part C and the curve above the data in part B represent the individual contributions of doublets 2 and 3, respectively.

Results

The majority of the samples we studied contained more than one chemical species. However, the CTD + benzoate sample was spectroscopically pure, and we discuss it first to illustrate our methodology. Then we present the results for the somewhat more complicated samples.

CTD + Benzoate. Benzoate is a weak inhibitor of CTD with a k_I of 10 mM at pH 7.5.[5b] Mössbauer spectra of CTD–benzoate recorded at 1.3 and 10 K are shown in Figure 1. Both spectra exhibit well-defined magnetic hyperfine interactions. The spectral components of all three Kramers doublets are at least partially resolved, a fact that allowed us to determine D and E/D independent of the EPR data. The 1.3 K spectrum is dominated by the contribution of doublet 1. The six-line pattern is typical of a high-spin ferric complex with a ground doublet having one EPR g value very much larger than the other two. From the six-line positions we calculate $H_{int} = -52.0 \pm 0.2$ T, $V_{zz} = -0.85$ mm/s and $\delta = 0.51$ mm/s. At 10 K the spectral components arising from doublets 2 and 3 are apparent. These two components are showm more clearly in the difference spectrum of Figure 1C. This spectrum was generated by subtracting the spectrum of Figure 1A from that of Figure 1B so as to cancel the ground doublet signal. The spectral component associated with doublet 2 is indicated by the solid line in Figure 1C while that of doublet 3 is indicated by the solid line above the data in Figure 1B. H_{int} for doublet 3 is 51.7 ± 0.4 T.

If the A tensor is isotropic, the ratio of the internal fields of doublets 1 and 3 must be equal to the ratio of the largest g value of the two doublets. This ratio of the internal fields is 1.01 ± 0.01 and suggests that $D < 0$ and $0.30 < E/D < 0.33$. The Mössbauer spectrum resulting from doublet 2 has a sharp right line and broad left line. Simulations show that a 5–10% anisotropy of the **g** tensor of doublet 2 would provide the proper shape. This condition is met by $0.30 \le E/D \le 0.31$. Fits to the data of Figure 1 and to

(12) Abbreviations used: salen, *N,N'*-ethylenebis(salicylideneamine); BzO, benzoate.
(13) Fujiwara, M.; Golovleva, L. A.; Saeki, Y.; Nozaki, M.; Hayaishi, O. *J. Biol. Chem.* **1975**, *250*, 4848–4855.
(14) Roe, A. L.; Schneider, D. J.; Mayer, R.; Pyrz, J. W.; Widom, J.; Que, L., Jr. *J. Am. Chem. Soc.* **1984**, *106*, 1676–1681.
(15) Que, L., Jr.; Mayer, R. *J. Am. Chem. Soc.* **1982**, *104*, 875–877.
(16) Lewis, J.; Mabbs, F. E.; Richards, A. *J. Chem. Soc. A* **1967**, 1014–1018.
(17) Pecoraro, V. L.; Wong, G. B.; Kent, T. A.; Raymond, K. N. *J. Am. Chem. Soc.* **1983**, *105*, 4617–4623.
(18) Münck, E. *Meth. Enzym.*, **1978**, *54*, 346–379.
(19) Abragam, A.; Bleaney, B. *Electron Paramagnetic Resonance of Paramagnetic Ions*; Claredon: Oxford, England, 1970.
(20) Oosterhuis, W. T. *Struct. Bonding (Berlin)* **1974**, *20*, 59–99.

Table I. EPR and Mössbauer Data for CTD Complexes and Analogues

CTD complex	g_{1x}[a] / g_{1y} / g_{1z}	g_{2x} / g_{2y} / g_{2z}	g_{3x} / g_{3y} / g_{3z}	δ, mm/s	$(eQ/2)V_{yy}$,[b] mm/s	$(eQ/2)V_{zz}$, mm/s	H_{int} of ground doublet, T
native I	...	4.25	...	0.45	−0.2		−50.7
	9.65	4.25	...				
	...	4.25	...				
native II	...	4.1	...	0.50			−54.0
	...	3.8	...				
	...	4.4	...				
catechol (sharp)	...	...	...	0.43	−0.45		−45.7
	9.6	...	...				
	...	...	...				
thiophenol	...	3.5	...	0.47		−0.82	−49.2
	...	4.2	9.12				
	9.86	5.0	...				
benzoate	...	4.25	...	0.51	+0.4	−0.85	−51.8
	9.64	4.15	...				
	...	4.30	...				
o-chlorophenol	...	4.25	...	0.46		−0.73	−50.6
	...	3.9	9.28				
	9.75	4.8	...				
phenol				0.46		−0.7	−50.5
pyrogallol + O_2	...	...	...	0.4			−47.5
	9.25	4.8	...				
	...	5.3	...				
Fe(salen)BzO	...	4.23	...	0.53	−0.69	+0.66	−50.0
analogue	9.59	4.19	...				
	...	4.31	...				

[a] EPR g values not observed are indicated by three dots. [b] V_{xx}, V_{yy}, and V_{zz} are the principal component of the electric field gradient. $V_{xx} + V_{yy} + V_{zz} = 0$.

Table II. Spin-Hamiltonian Parameters for CTD Complexes and Analogues

CTD complex	D, cm^{-1}	E/D[a]	ΔE_Q,[a] mm/s	η	$A/g_n\beta_n$, T
native I	+0.7 ± 0.3	0.33			−21.0
native II	−0.4 ± 0.3	0.28			−21.6
catechol	+2.0	0.32			−18.9
thiophenol	−1.6	0.22	−0.92	−1.0 ± 0.3[b]	−20.0
benzoate	−0.8 ± 0.3	0.31	−0.85	0	−21.5
o-chlorophenol	−1.0	0.23			−20.8
phenol	−1.0	0.23			−20.8
pyrogallol + O_2	+1.9	0.21			−20.9
Fe(salen)BzO	+1.2	0.31	+0.78	+1.0	−20.9

[a] $\Delta E_Q = (eQV_{zz}/2)(1 + \eta^2/3)^{1/2}$ where $\eta = (V_{xx} - V_{yy})/V_{zz}$. [b] Determined from the shape of Mössbauer spectral component of doublet 2.

a 4.2 K spectrum (data not shown) yield $D = -0.8 \pm 0.3$ cm^{-1} and $A/g_n\beta_n = -21.5 \pm 0.1$ T.

For $D < 0$ and $E/D = 0.31$, eq 1 yields $g_{1z} = 9.73$, $g_{2x} = 4.27$, $g_{2y} = 4.15$, $g_{2z} = 4.42$, and $g_{3y} = 9.61$. The EPR spectrum of a CTD + benzoate sample with ^{57}Fe in natural abundance is shown in Figure 2A. The observed g values are at 9.64, 4.31, and 4.17. No other features were observed around 9.7 between 2.4 and 15 K. Evidently, the resonance from doublet 3 overlaps the 9.64 peak of the ground doublet. Considering our assumptions that $g_0 = 2$ and that $\tilde{\mathbf{A}}$ is isotropic, the agreement between the Mössbauer and EPR data is good. The EPR and Mössbauer results are listed in Tables I and II.

Native CTD. Quite unexpectedly the Mössbauer spectra of native CTD revealed two distinct species. Therefore, we investigated native CTD under eight different conditions (H_2O, pH 6.5; 50 mM Tris OAc, pH 7.3, 7.8, and 8.3; 50 mM HEPES, pH 6.7, 7.8, and 8.3; 20% (v/v) glycerol/50 mM HEPES, pH 7.5). In all cases, two major components were obtained and efforts to obtain only one major component in a native enzyme sample failed. Figure 3A shows the Mössbauer spectrum of native CTD in HEPES buffer, pH 8.3. Species I exhibits well-resolved EPR features at $g = 9.65$ and 4.25 as shown in Figure 2B. The corresponding Mössbauer spectral component (indicated by the solid line in Figure 3A) accounts for ~60% of the total Fe and has parameters nearly identical with those of *B. fuscum* protocatechuate 3,4-dioxygenase ($H_{int} = -50.7$ T). Species II, on the other hand, has $H_{int} = -54.0$ T. EPR signals at $g = 4.4$, 4.1, and 3.8 attributable to doublet 2 of species II are observed and suggest $E/D = 0.28$. Its ground doublet EPR signal is not resolved. The large H_{int} and the absence of a low-field EPR signal suggest that $D < 0$ and $g_{1z} \geq 9.8$. Species II accounts for ~25% of the total Fe in the sample. The values quoted in Table II for D for native species 1 and 2 have large relative uncertainties. These arise from the poor resolution of the two species in the Mössbauer spectra.

Approximately 15% total Fe is unaccounted for by species I and II. This third type of iron yields the broad adsorption beneath the simulation at −6 and +7 mm/s in Figure 3A. If the A of this iron type is typical, then the small hyperfine splitting indicates that the ground doublet **g** tensor is not severely anisotropic, i.e. E/D is significantly less than $^1/_3$. (The 13 mm/s splitting corresponds to $H_{int} = -4.0$ T and, assuming $A/g_n\beta_n = -21$ T, an EPR g value of $g_{1y} = 7.6$.) The EPR signal of this material should be relatively strong. Indeed a very broad signal is observed on the high-field side of the $g = 9.65$ peak in Figure 2B. Such a broad EPR signal is observed at much lower intensities in all the complexes discussed below.

Samples prepared in other solvents and at different pH values displayed the same spectral components although the relative amounts of the components varied. For example, in H_2O at pH 6.5 about 25% of the iron was present as species I. The sample in 20% glycerol/150 mM HEPES pH 7.5 was the most homogeneous with ~70% total Fe appearing as species I.

CTD + Phenols. Phenols, being substrate analogues, are competitive inhibitors of CTD. Mössbauer spectra for both the CTD–phenol and the CTD–*o*-chlorophenol complexes have been obtained and they are virtually superimposable. Thus, only the *o*-chlorophenol complex will be discussed.

An EPR spectrum of an ^{57}Fe-enriched sample of the CTD–*o*-chlorophenol complex is shown in Figure 2C. The low-field resonance at $g = 9.75$ is clearly distinct from the $g = 9.65$ native signal. However, the broad tail to the high-field side of $g = 9.75$ indicates that some native material is present. Together with the $g = 4.25$ and $g = 4.1$ signals, these data suggest that all three of the native species are present.

Because of the noticeable line broadening due to magnetic hyperfine interactions, the EPR features of the CTD–*o*-chlorophenol complex are better illustrated by the spectra of a sample

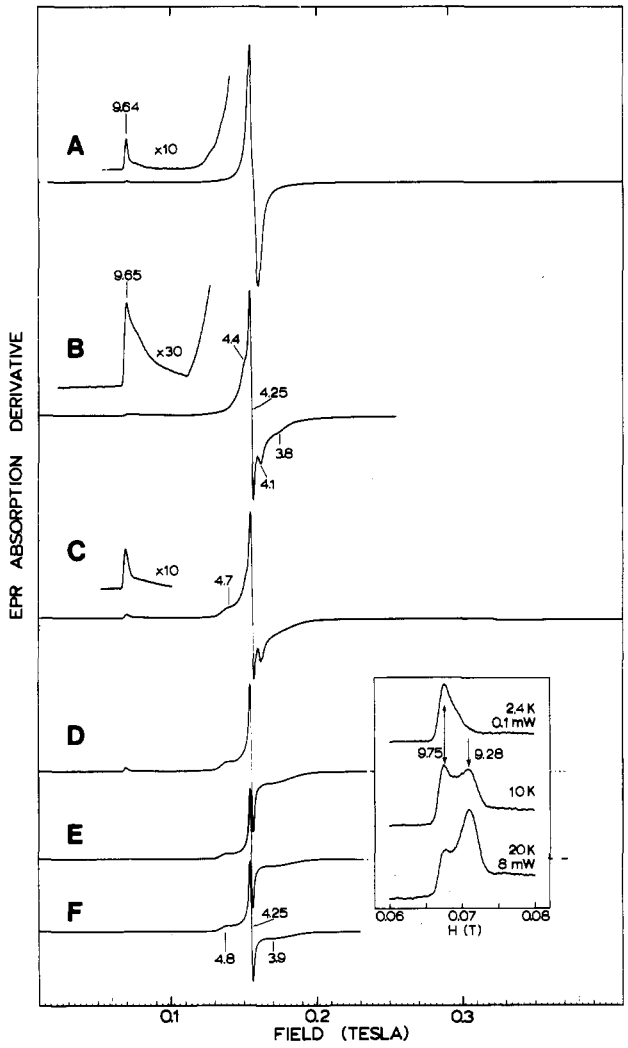

Figure 2. EPR spectra of (A) ^{57}Fe CTD + benzoate (100 mM) at 4.8 K, (B) ^{57}Fe CTD at 4.3 K, (C) ^{57}Fe CTD + *o*-chlorophenol (10 mM) at 3.6 K, and ^{56}Fe CTD + *o*-chlorophenol (10 mM) at (D) 2.4, (E) 10, and (F) 20 K. The insert shows the low-field region of the ^{56}Fe CTD + *o*-chlorophenol spectra at the temperatures indicated. Experimental conditions: microwave frequency, 9.22 GHz; modulation amplitude, 1 mT, modulation frequency, 100 kHz; 50 mM HEPES (pH 7.5); microwave power, 0.2 mW except where indicated.

not enriched in ^{57}Fe. The data in Figure 2D–F have significantly weaker native signals. The 10 and 20 K spectra show a nicely resolved excited state signal at $g = 9.28$. This signal was not observed for any native sample at similar temperatures. The $g_{3y} = 9.28$ signal plus the ground state $g_{1z} = 9.75$ resonance suggest $D < 0$ and $E/D = 0.23$. These parameters also correlate well with the $g = 4.8$, 4.25, and 3.9 resonances observed for doublet 2.

The presence of some native material in the sample of Figure 2C is confirmed by Mössbauer spectra (primarily by absorption at +9 mm/s by native component 2). Roughly 10–20% total Fe appears to be in the native form. Figure 3B shows a difference spectrum obtained by subtracting from the raw data the 4.2 K spectrum of the native sample of Figure 3A scaled to 20% total Fe. This difference spectrum and others recorded at 1.3, 10, and 20 K were fitted well with the parameters listed in Table II.

CTD + Thiophenol. In the course of our investigation, we studied the interaction of thiophenol with CTD. Thiophenol is a good competitive inhibitor of CTD ($K_i = 20$ μM). The CTD–thiophenol complex exhibits a visible spectrum with absorbance maxima near 385 and 470 nm and an extinction coefficient nearly twice that of the benzoate complex. Titration experiments show that one thiophenol binds per CTD molecule and resonance Raman experiments show that the tyrosine ligands remain coordinated upon thiophenol binding (data not shown). The data taken collectively suggest that thiophenol binds to the ferric center.

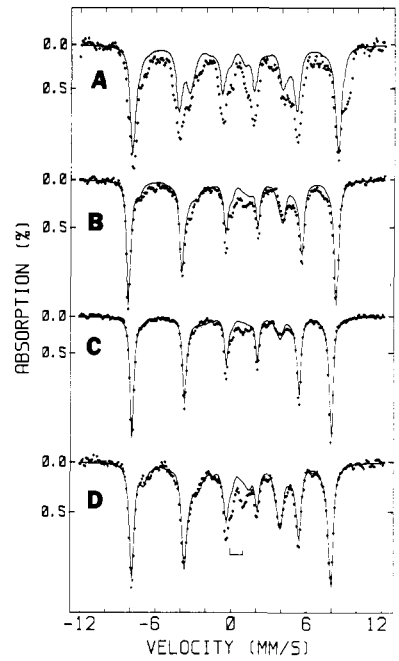

Figure 3. Mössbauer spectra of CTD complexes in 50 mM HEPES (pH 7.5) buffer in a 0.06-T parallel field with simulations (solid lines) calculated from eq 1 and 3 and the parameters of Tables I and II plotted with areas quoted relative to the displayed data: (A) native CTD (pH 8.3) 1.3 K spectrum for theory with $D = 0.4$ cm^{-1} for component I only plotted at 60% (see text); (B) CTD + *o*-chlorophenol (10 mM) 4.2 K spectrum after subtraction of native CTD spectrum scaled to 20% total Fe with theory plotted at 80%; (C) CTD + thiophenol (5 mM) 4.2 K spectrum after subtraction of native CTD spectrum scaled to 15% total Fe with theory plotted at 87%; (D) CTD + thiophenol (5 mM) 10 K spectrum with data and theory prepared as in part C.

Analysis of the Mössbauer and EPR data for the CTD-thiophenol complex reveals that ~75% total Fe is associated with the thiophenol complex, ~15% is in the native form, and ~10% is unidentified material. The 3.4 K EPR spectrum (Figure 4A) shows a $g = 9.86$ ground-state signal with a 2.5-mT line width. The broad absorption arises from native protein. At 10 K (Figure 4B) an excited-state resonance at $g = 9.12$ with a 3.0-mT line width is observed. Resonances also appear at $g = 5.0$ and 3.5 for the thiophenol complex with additional resonances at ~4.3 observed for the native component. The observed thiophenol–CTD g values are fitted nicely with $E/D = 0.22$ and $D < 0$. The presence of a native component prevented the determination of $|D|$ from the intensities of 9.83 and 9.10 EPR signals. Mössbauer spectra of the thiophenol–CTD complex, shown in Figures 3C,D, are fitted well with $D = -1.6$ cm^{-1}, $E/D = 0.22$ and $A/g_n\beta_n = -20.0$ T.

In this sample, approximately 6% of total Fe is associated with a quadrupole doublet with $\Delta E_Q \simeq 0.9$ mm/s and $\delta = 0.5$ mm/s (indicated by the bracket in Figure 3D). This material is most likely a high-spin ferric complex that is aggregated. The presence of magnetically dilute, fast-relaxing high-spin material could not explain this component since the doublet is not measurably broadened by an 0.06-T applied field at $T = 1.3$ K. Spectral simulations show that, under these conditions, a fast-relaxing $S = {}^5/_2$ paramagnet would exhibit substantial broadening ($g\beta H_{app}/kT = 0.3$).

CTD + Catechol. The binding of catechol to CTD produced a sharp Mössbauer component with an unusually small H_{int} for a ferric complex with non-sulfur ligands. Figure 5A shows the raw data of CTD + catechol superimposed with those of native CTD. The primary result of catechol binding is the disappearance of native component I and the appearance of a sharp component with $H_{int} = -45.7$ T. A spectrum recorded at 4.2 K with 0.06-T perpendicular field (data not shown) was significantly different from that recorded in parallel field. We also observed at 10 K an additional Mössbauer component with $H_{int} = 53.0$ T attributable to an excited electronic doublet.

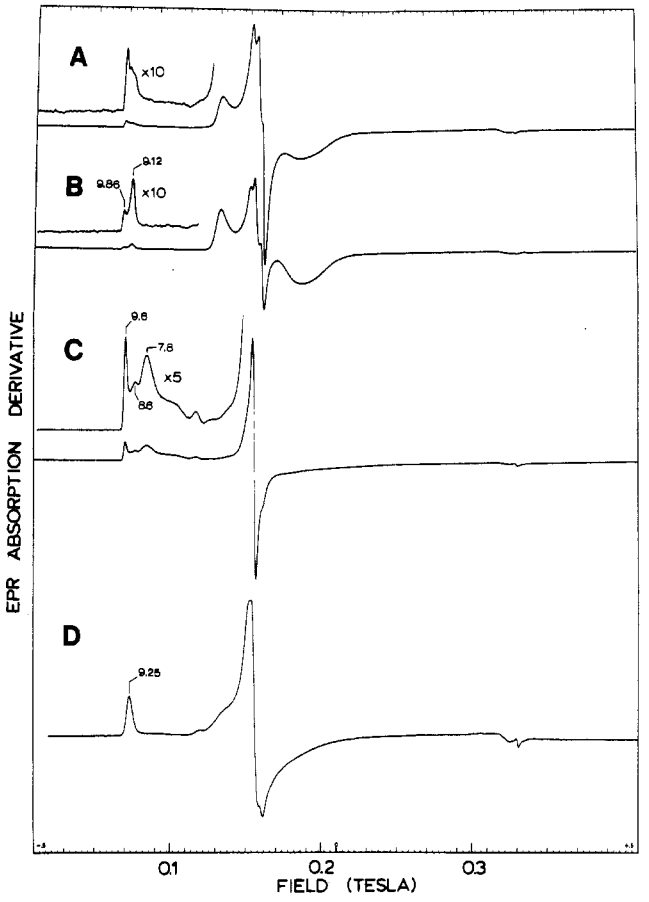

Figure 4. EPR spectra of CTD complexes in 50 mM HEPES (pH 7.5) buffer; (A) CTD + thiophenol (5 mM), 3.4 K; (B) CTD + thiophenol (5 mM), 10 K; (C) CTD + catechol (10 mM), 2.4 K; (D) CTD + pyrogallol (10 mM), 2.7 K. Experimental conditions were as quoted in Figure 2.

The EPR spectrum of the catechol complex is shown in Figure 4C. There are broad peaks at $g = 8.6$ and $g = 7.8$. However, integration of the spectrum shows that roughly half the total Fe is associated with the $g = 9.6$ resonance while the other half has signals distributed fairly evenly between $g = 9.6$ and $g = 6$. No significant fraction of the Fe resonates at $g = 8.6$ or 7.8.

The spectrum of the catechol complex is best seen in Figure 5B where we have attempted to remove the native components (see Discussion). The simulation shown in Figure 5B is sum of four spectral components. The major component is the sharp component with parameters as quoted in Tables I and II. It accounts for 50% of the area of the plotted simulation (i.e. 40% total Fe of the sample). The other three represent the material giving rise to the broad EPR signal. The three parameter sets were $A/g_n\beta_n = -21.5$ T, $D > 0$, and $E/D = 0.05$, 0.1, and 0.18. These three components each account for one-sixth of the area of the plotted simulation. Both the significant field direction dependence of the Mösbauer data and the complex EPR spectrum are explained well with such composite simulations. The observed excited-state signal with $H_{int} = -53.0$ T arises from the same iron sites that yield the broad EPR ground-state signal.

CTD + Pyrogallol + O_2. Rapid kinetic studies of the reaction of the CTD–pyrogallol complex with O_2 have shown the presence of two intermediates.[15] At 0 °C, the second intermediate can be generated under steady-state conditions to afford a substantial concentration of the desired complex. A Mössbauer sample of the steady-state intermediate was obtained with 0.5 mM CTD. Native material accounted for 25% ± 5% of the total Fe of the sample. Subtraction of the native spectral component (using the 4.2 K spectrum of the sample of Figure 5A) yields the difference spectrum in Figure 5C. This component is assigned to the steady-state intermediate. (The proportion of steady-state intermediate in the sample depends on the relative concentrations

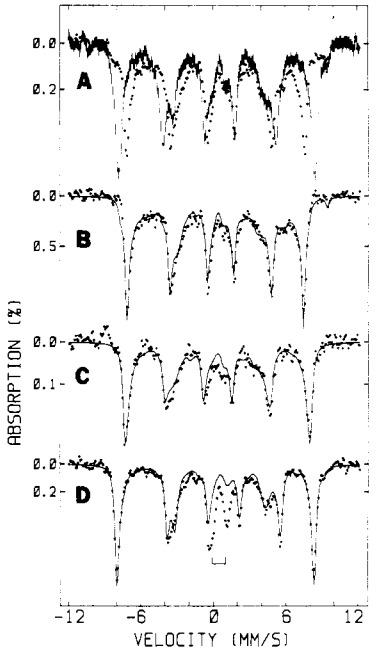

Figure 5. Mössbauer spectra recorded with a 0.06-T parallel field and $T = 4.2$ K with simulations (solid lines) prepared as described in Figure 3. (A) Spectrum of CTD + catechol (10 mM) (points) compared with spectrum of native CTD (hatchmarks). Spectra were plotted with equal areas. Both samples were in 50 mM HEPES (pH 7.5) buffer and contained 20% (v/v) glycerol. (B) Spectrum of CTD + catechol. Spectrum was prepared by subtracting the native CTD spectrum scaled to 20% total Fe. Multicomponent simulation was as described in text and plotted at 100%. (C) Spectrum of CTD + pyrogallol + O_2 after subtraction of native CTD spectrum scaled to 25% total Fe. Simulation was plotted at 100%. (D) Spectrum of Fe(salen)BzO in 9:1 toluene/CH_2Cl_2 solution. Simulation was plotted at 85%.

of enzyme and O_2. More concentrated enzyme solutions gave rise to a smaller proportion of intermediate trapped under the conditions used to prepare the samples. The 0.5 mM concentration used was a compromise between signal intensity and fraction of intermediate trapped.)

The presence of native material in the sample is confirmed by the EPR spectrum of the Mössbauer sample (Figure 4D), which shows a sharp $g = 4.3$ signal and a downward peak at $g = 4.1$. The intermediate exhibits a broad but well-defined ($\Gamma = 4$ mT) signal at $g = 9.25$ as well as broad and partially resolved features at $g = 5.3$ and 4.8. The EPR data suggest a distribution of species with $D > 0$ and $0.17 \leq E/D \leq 0.25$. The Mössbauer spectrum (after subtraction of the native components) of the intermediate also suggests a heterogeneous sample.

A simulation with $E/D = 0.21$ and $A = -20.9$ T accounts for the essential features of the ground-state Mössbauer spectrum. However, the observed outer lines of the magnetic pattern require an intrinsic line width of $\Gamma = 0.4$ mm/s. A simulation of similar quality can be obtained by summing three spectra calculated with $E/D = 0.17$, 0.21 and 0.25 and $\Gamma = 0.3$ mm/s. These were weighted 8:10:4, respectively, as suggested by the shape of the $g = 9.25$ feature of the EPR spectrum. The single component simulation with $\Gamma = 0.4$ mm/s is plotted over the data at 75% total area. The relative populations of the ground and middle doublets at 4.2 K were determined to be 85/15, which yields $D = \sim+1.9$ cm^{-1} for this intermediate.

Fe(salen)BzO. In the course of our investigations of models for the catechol dioxygenases, we studied the Mössbauer and EPR properties of Fe(salen)BzO. This complex is conveniently produced by the addition of benzoic acid to $[Fe(salen)]_2O$. Spectrophotometric studies indicate that the mononuclear complex is formed in solution,[21] although the complex is probably a weakly

(21) Heistand, R. H., II; Lauffer, R. B.; Fikrig, E.; Que, L., Jr. *J. Am. Chem. Soc.* **1984**, *106*, 1676–1681.

coupled dimer in the solid state.[22] Fe(salen)BzO exhibits an EPR spectrum typical of high-spin Fe(III) in a rhombic environment ($E/D \sim 0.31$). Its Mössbauer spectra (Figure 5D) are also consistent with this interpretation and yield $A/g_n\beta_n = -20.9$ T and $D = +1.2$ cm^{-1}. Interestingly, the A value is characteristic of the *B. fuscum* component of native CTD and those of the PCD's.[7,8] This suggests that the Fe(salen)BzO coordination resembles the active site of these enzymes. As indicated by the bracket in Figure 5D, a quadrupole doublet accounting for ~10% total Fe is also observed. The parameters $\Delta E_Q = 1.1$ mm/s and $\delta = 0.5$ mm/s suggest that residual, diamagnetic $[Fe(salen)]_2O$ dimer was present.[23]

Discussion

Table II summarizes the spin-Hamiltonian parameters derived from the simulations of the Mössbauer spectra of the complexes studied. For all complexes studied, the iron center retains its high-spin ferric oxidation state, but exhibits differing D and A values.

The native enzyme consistently exhibited two major Mössbauer components, despite efforts to generate a homogeneous sample by altering pH and buffers. The relative amounts of the two components do vary with conditions employed, but the changes observed are not systematic enough to allow conclusions to be drawn. One of the components observed in the Mössbauer spectrum of the native enzyme exhibits magnetic hyperfine parameters virtually identical with those of native protocatechuate 3,4-dioxygenase (PCD) from *P. aeruginosa*[7] and *B. fuscum*.[8] Though the D value for CTD is somewhat smaller, the E/D and A values are nearly identical with those observed for the PCD's. When compared to other non-heme iron complexes,[20,24,25] the $A/g_n\beta_n$ value of −21.0 T appears unique to the dioxygenases. The second component in the spectrum of the native enzyme has a $A/g_n\beta_n$ value of −21.6 T and has somewhat broader features than the PCD-like component. The two components are clearly different and must reflect different coordination environments of the ferric center.

The value of A is a measure of the hyperfine interaction of the iron electrons with the ^{57}Fe nucleus and thus reflects the covalency of the metal–ligand bonds. Transferrin, enterobactin, and $[Fe(EDTAH)H_2O]$ all exhibit $A/g_n\beta_n = -22$ T, reflecting octahedral oxygen–nitrogen environments,[20] while the tetrahedral sulfur-coordinated rubredoxin and desulforedoxin exhibit values near −16 T.[24,25] In the course of our studies, we examined the Mössbauer spectra of ^{57}Fe(salen)BzO, a complex with a coordination environment consisting of two phenolate oxygens, two imine nitrogens, and a carboxylate. The A value obtained for this complex, nearly matches those observed for native PCD from *P. aeruginosa* and *B. fuscum* and for the PCD-like component in native CTD. This suggests that the active site for the dioxygenases may resemble the coordination environment of Fe(salen)BzO. Indeed, the details of the dioxygenase active site derived from other spectroscopic methods approximate the environment in Fe(salen)BzO. Resonance Raman spectroscopy has demonstrated the presence of two coordinated tyrosines (two phenolates),[5b,26] while EXAFS studies suggest the participation of histidine (imine N).[27] Though there is currently no evidence for carboxylate binding in the native enzymes, the effect of the coordinated water in the active site of these enzymes[28] is perhaps mimicked by the benzoate ligand in the model complex. Similar A values are also found for the CTD–phenol complexes and the steady-state intermediate derived from the reaction of the CTD–pyrogallol complex with O_2.

The binding of ligands to the enzyme appears to transform the two components of the enzyme into one dominant form, as if the ligand locks the ferric center in a particular environment. A similar sharpening of spectral features has also been observed in the resonance Raman spectra of CTD–inhibitor complexes.[5b] The features associated with tyrosine C–O stretching in the spectrum of the native enzyme appear broad, suggestive of multiple components, while those for the benzoate and the phenol complexes are resolved into two components that have been assigned as the ν_{CO}'s of the two tyrosines coordinated to the ferric center.

The values for A, D, and E/D vary from complex to complex.[29] Similar variations in A are observed for analogous complexes of *B. fuscum* PCD,[8,30] with the exception of the catechol complexes. A comparison of the phenol and thiophenol complexes shows that substituting an oxygen with sulfur in the iron coordination sphere results in a decrease of 0.8 T in the value of A, indicating the greater covalency of the Fe–S bond. This relatively small decrease in A suggests that the large decreases in A noted for rubredoxin[24] and desulforedoxin[25] are associated not only with the presence of thiolate sulfur but also with other factors such as the tetrahedral coordination.

Differences in the spin-Hamiltonian parameters for the phenol and catechol complexes are striking. The A value of the latter, in particular, is the smallest in magnitude of all the dioxygenase complexes studied thus far and indicates a greater delocalization of unpaired spin density away from the metal and presumably onto the catechol. ^{1}H NMR studies have shown that the catechol is coordinated as a phenol in the CTD–substrate complex, i.e. only one oxygen is coordinated to the ferric center.[31] Thus the difference in the A values of the phenol and the catechol complexes would suggest that the active site undergoes a significant change as it binds substrate. The greater delocalization of unpaired spin density onto the substrate could serve to enhance the reactivity of substrate to dioxygen.

The parameters for the ES complex of CTD are also distinct from those for the catechol complex of *B. fuscum* PCD.[30] The CTD complex has $A/g_n\beta_n$ of −18.9 T, while the PCD complex exhibits −20.2 T. This may reflect the differences in the coordination mode of catechol to the ferric center in the two enzymes, as shown by NMR studies.[31]

In summary, the Mössbauer data on CTD and its various complexes confirm the conclusion reached by studies on PCD,[7,8] namely that the iron center retains its high-spin ferric character in all the complexes studied thus far. These observations are in agreement with the persistence of the tyrosinate-to-iron(III) charge-transfer band observed in these complexes as well as in intermediates observed in transient kinetic experiments.[9,10] These observations lend further credence to the substrate activation mechanism, which has been proposed to accommodate these observations.[11] The significant difference of the Mössbauer pa-

(22) Wollman, R. G.; Hendrickson, D. N. *Inorg. Chem.* **1978**, *17*, 926–930.
(23) Murray, K. S. *Coord. Chem. Rev.* **1974**, *12*, 1–35.
(24) Debrunner, P. G.; Münck, E.; Que, L., Jr.; Schulz, C. E. In *Iron-Sulfur Proteins*; Lovenberg, W. E., Ed., Academic: New York, 1977; Vol. 3, pp 381–417.
(25) Moura, I.; Huynh, B. H.; Hausinger, R. P.; LeGall, J.; Xavier, A. V.; Münck, E. *J. Biol. Chem.* **1980**, *255*, 2493–2498.
(26) Que, L., Jr.; Epstein, R. M. *Biochemistry* **1981**, *20*, 2545–2549.
(27) Felton, R. H.; Barrow, W. L.; May, S. W.; Sowell, A. L.; Goel, S.; Bunker, G.; Stern, E. A. *J. Am. Chem. Soc.* **1982**, *22*, 6132–6134.
(28) Whittaker, J. W.; Lipscomb, J. D. *J. Biol. Chem.* **1984**, *259*, 4487–4495.

(29) As noted above, the relative amounts of the several native spectral components varied with pH and buffer. This situation complicates the interpretation of the spectra of the catechol, pyrogallol, thiophenol, and chlorophenol CTD complexes. Both the EPR and Mössbauer data indicated that nativelike components were present in the ^{57}Fe-enriched, ligand-bound forms at the 10–20% level. In order to evaluate the major spectral component of each sample, we had to remove the nativelike signals. As a first-order correction, we subtracted the appropriate spectrum of the native CTD sample with HEPES at pH 8.3. The amount subtracted was adjusted to cancel the most prominent native feature, namely the broad peak at +9 mm/s. If the ratios of native components I and II were not the same in the ligand-bound sample and the native sample, then this subtraction is not correct. The magnitude of the artifacts introduced is best seen in the spectrum of the CTD–catechol complex. No evidence of native component I can be seen in the raw data (Figure 5A). However, component II is clearly present. Subtraction of the native spectrum scaled to 20% total Fe cancels component II. The small glitches at −6.8 and +8.5 mm/s in Figure 5B arise from subtracting too much of native component I. These artifacts are just slightly larger than the noise and, thus, do not seriously affect our analysis.

(30) Kent, T. A.; Whittaker, J. W.; Lipscomb, J. D.; Münck, E., unpublished observations.
(31) Lauffer, R. B.; Que, L., Jr. *J. Am. Chem. Soc.* **1982**, *104*, 7324–7325.

rameters of the CTD–catechol complex relative to the other complexes may signal such an activation, which affords a substrate molecule capable of reacting with dioxygen directly. That such a mechanism is chemically reasonable is supported by recent observations of iron(III)-catalyzed cleavage of catechols in chemical systems.[32,33]

Acknowledgment. This work was supported by the National Institutes of Health (Grant GM 22701-10, E.M.; Grant GM-33162, L.Q.). L.Q. is an Alfred P. Sloan Research Fellow (1982–1986) and an NIH Research Career Development Awardee (1982–1987). We thank Dr. P. Nizin for collecting the Fe(salen)BzO data.

(32) White, L. S.; Nilsson, P. V.; Pignolet, L. H.; Que, L., Jr. *J. Am. Chem. Soc.* **1984**, *106*, 8312-8313.

(33) Weller, M. G.; Weser, U. *J. Am. Chem. Soc.* **1982**, *104*, 3752-3754.

Contribution from the Chemistry Division, Argonne National Laboratory, Argonne, Illinois 60439, and Institut für Radiochemie, Technische Universität München, 8046 Garching, West Germany

Rates of Oxidation of Selected Actinides by Cl_2^- †

Christoph Lierse,‡ James C. Sullivan,*§ and Klaus H. Schmidt§

Received September 26, 1986

The Cl_2^- radical produced by pulse radiolysis of aqueous sodium chloride solutions oxidizes U(V), Np(V), Pu(III), and Am(III). The respective rates (M^{-1} s^{-1}) are $(6.5 \pm 2) \times 10^8$, $(2.38 \pm 0.10) \times 10^6$, $(4.8 \pm 0.4) \times 10^7$, and $(3.2 \pm 0.4) \times 10^5$. The mechanism for the oxidation of U(V) and Np(V) is discussed in terms of the Marcus theory. There is an unexpected linear free energy correlation with the measured rate parameters in the oxidation of U(III), Ti(III), Pu(III), and Am(III).

The pulse radiolysis studies of actinide ions in aqueous solutions[1] have been concerned, predominantly, with the reactions of the primary radicals e_{aq}^- and OH. The salient exception is the study of the reduction of the carbonate radical ion[2] by the carbonato complexes of U(V), Np(V), and Pu(V). That study, as well as the present, was motivated in part to determine if a linear free energy relationship provides an adequate summary of the data over the ranges $\Delta G°$ and log k associated with such reactions. To that end, the present study examines the rates of oxidation of trivalent and pentavalent actinide ions in sodium chloride solutions by the Cl_2^- radical[3] produced by pulse radiolysis techniques. An additional aspect of the present investigation is the attempt to delineate feasible mechanisms for the disappearance of Cl_2^- since the mechanisms[4] of such reactions have not been completely elucidated.

Experimental Section

A stock solution of NaCl (Suprapure, Merck Co., No. 6406) was prepared by the dissolution of weighed quantities of the salt in triple-distilled water. Stock solutions of HCl and NaOH were prepared by dilution of concentrated reagent grade solutions and standardized by conventional techniques. The U(VI) stock solution was prepared by dissolution of a weighed quantity of NBS U_3O_8. The ^{237}Np(V) stock solutions were prepared by dissolution of freshly precipitated neptunium(V) hydroxide and assayed spectrophotometrically by using the peak at 980 nm (ϵ = 404 M^{-1} cm^{-1}). The ^{242}Pu(III) stock solution was prepared by electrolytic reduction of Pu(VI) at a Pt electrode and assayed at 560 nm (ϵ = 38 M^{-1} cm^{-1}). The ^{243}Am(III) solutions were freshly prepared immediately prior to the pulse radiolysis studies (after precipitation as the hydroxide and subsequent washes with triply distilled water) and standardized spectrophotometrically at 503 nm (ϵ = 450 M^{-1} cm^{-1}).

The U(VI) and Np(V) solutions were adjusted to the proper pH by the previously described[5] syringe technique by adding appropriate quantities of HCl or NaOH. The pH of the Pu(III) and Am(III) solutions was adjusted by removing H^+ electrochemically in a special device shown in Figure 1. For all pH measurements, a ROSS electrode (Orion Co.) with 3 N NaCl as filling solution was used.

Pulse radiolysis was carried out with a beam of 15 MeV electrons at 4–40-ns pulse length. Absorption spectra of the transient species, generated by irradiation of the solutions with single pulses of high-energy electrons, were obtained by the streak camera–tv scanning method described previously.[6] The irradiation procedure and dose measurements were essentially as described earlier.[7] Some of the rate data were obtained by photomultiplier techniques, where the output was digitized in a Biomation 8100 transient recorder and stored in a LSI 11/23 computer. The digital data were then transferred over a local area network to a VAX 11/780 computer, where the data were analyzed.[8] In some cases, a kinetic model program[9] was used to simulate the optical transient, and the simulated signal was compared with the experimental curve.

Results

A. $U(V) + Cl_2^- \rightarrow U(VI) + 2Cl^-$. Since U(V) in solution is not stable, it was produced in situ by reduction of U(VI) by the hydrated electron. We irradiated a He-saturated solution of 10^{-2} M $UO_2(ClO_4)_2$ containing 1 M NaCl, at pH 3, with a pulse of electrons. The following sequence of reactions then occurs:

$$H_2O \rightsquigarrow e_{aq}^-, H, OH \quad (0)$$

$$e_{aq}^- + UO_2^{2+} \rightarrow UO_2^+ \quad (1)$$

$$e_{aq}^- + H^+ \rightarrow H \quad (2)$$

$$OH + Cl^- \rightleftarrows ClOH^- \quad (3)$$

$$ClOH^- + H^+ \rightleftarrows Cl + H_2O \quad (4)$$

$$Cl + Cl^- \rightleftarrows Cl_2^- \quad (5)$$

$$Cl_2^- + UO_2^+ \rightarrow UO_2^{2+} + 2Cl^- \quad (6)$$

$$Cl_2^- + H \rightarrow H^+ + 2Cl^- \quad (7)$$

$$Cl_2^- + Cl_2^- \rightarrow Cl_3^- + Cl^- \quad (8)$$

$$H + H \rightarrow H_2 \quad (9)$$

At its absorption peak at 340 nm, Cl_2^- is the only strongly ab-

† Work performed under the auspices of the Office of Basic Energy Sciences, Division of Chemical Science, U.S. DOE, under Contract No. W-31-109-ENG-38.

‡ Technische Universität München.
§ Argonne National Laboratory.

(1) See for example: Sullivan, J. C.; Gordon, S.; Cohen, D.; Mulac, W. A.; Schmidt, K. H. *J. Phys. Chem.* **1976**, *80*, 1684.
(2) Mulac, W. A.; Gordon, S.; Schmidt, K. H.; Wester, D.; Sullivan, J. C. *Inorg. Chem.* **1984**, *23*, 1639.
(3) Jayson, G. G.; Parsons, B. J.; Swallow, A. J. *J. Chem. Soc., Faraday Trans. 1* **1973**, *169*, 1597.
(4) Golub, D.; Cohen, H.; Meyerstein, D. *J. Chem. Soc., Dalton Trans.* **1985**, 641.
(5) Hart, E. J.; Anbar, M. *The Hydrated Electron*; Wiley-Interscience: New York, 1970.
(6) Schmidt, K. H.; Gordon, S.; Mulac, W. A. *Rev. Sci. Instrum.* **1976**, *47*, 356. Schmidt, K. H.; Gordon, S. *Rev. Sci. Instrum.* **1979**, *50*, 1656.
(7) Gordon, S.; Schmidt, K. H.; Hart, E. J. *J. Phys. Chem.* **1977**, *81*, 104.
(8) The nonlinear least-squares fitting program used for rate parameter determination was written by Charles D. Jonah, Chemistry Division, Argonne National Laboratory.
(9) Schmidt, K. H. *Argonne Natl. Lab.*, [Rep.] *ANL* **1966**, *ANL-7199*; **1970**, *ANL-7693*. These programs were modernized and adapted to the VAX 11/780 in 1986.

0020-1669/87/1326-1408$01.50/0